ACS OMEGA

Article

Cite This: ACS Omega 2018, 3, 10589−10600

http://pubs.acs.org/journal/acsodf

Hydrogen Bonding as a Clustering Agent in Protic Ionic Liquids: Like-Charge vs Opposite-Charge Dimer Formation

Andrea Le Donne, Henry Adenusi, Francesco Porcelli, and Enrico Bodo*

Chemistry Department, University of Rome "La Sapienza", Piazzale Aldo Moro 5, 00185 Rome, Italy

Supporting Information

ABSTRACT: The local structure of a series of homologous protic ionic liquids (PILs) is investigated using ab initio computations and ab initio-based molecular dynamics. The purpose of this work is to show that in PILs the network of hydrogen bonds may promote like-charge clustering between anionic species. We correlate the theoretical evidence of this possibility with viscosity experimental data. The homologous series of liquids is obtained by coupling choline with amino acid anions and varying the side chain. We find that the frictional properties of the liquids are clearly connected to the ability of the side chain to establish additional hydrogen bonds (other than the trivial cation−anion interaction). We also show that the large variation of bulk properties along the series of compounds can be explained by assuming that one of the sources of friction in the bulk liquid is the like-charge interaction between anions.

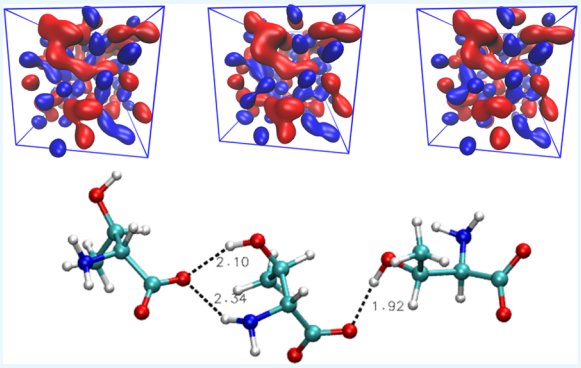

1. INTRODUCTION

Protic ionic liquids (PILs)[1−4] are among the most interesting members of the rather vast class of materials known as ionic liquids (ILs). PILs can be formally thought (and often practically synthesized) as the result of an acid−base reaction. If the complexity of the molecular constituents is sufficient, lattice formation is frustrated by entropic effects and occurs only at low temperatures, so that the resulting material is liquid under room conditions. In practice, lattice formation at room temperature can be prevented rather easily using molecular ions with delocalized charge distributions (weakening of electrostatic interactions) or with a sufficient difference in their volumetric dimensions and shapes (disorder induced by steric mismatch).

It is well known that only a large difference in the pK_a's of the reagents (>6) in the acid−base reaction guarantees the ensuing liquid to be completely ionized.[5] If the difference in pK_a is small (<4),[6] the liquid may turn out to be a mixture of ions and polar molecules, where phase separation and evaporation of the volatile component may occur to various degrees.

Despite their synthetic simplicity, PILs show unexpectedly complex structural patterns and even some intriguing chemical activity, which are due to a series of interrelated phenomena, such as nanosegregation[7,8] and hydrogen bonding features,[9,10] and due to the possibility of having tautomerization reactions involving secondary protic functions on the molecular structure.[11,12]

Due to the possibility of changing the substituent on either the cation (base) or the anion (acid), the number of possible PILs is practically infinite, and it should be possible to tune their physical and chemical properties by engineering the desired cation−anion structures. Particularly attractive is the possibility of creating a homologous series of materials to rationalize the relation between the molecular structure and the ensuing bulk properties.[13] In this work, we will use such a series of compounds where the same choline cation [Ch] is coupled to a (singly) deprotonated amino acid anion [AA], whose variety is obtained by changing the side chain (for a complete list of the liquids under investigation see Figure S1 in the Supporting Information).

Incidentally, it turns out that these compounds (which have been actually synthesized)[14] are fully biocompatible[15−17] and might be appealing for applications in pharmacological and biomedical research.[18−23] In addition, these PILs, often possessing relatively mobile protons on the side chain, have been a target of intensive research in electrochemical applications.[24−27]

The aim of this work is to elucidate the short-range structure of the bulk fluids by using both newly computed ab initio data and the results of previously performed ab initio molecular dynamics (AIMDs) simulations. One of the most intriguing features that we have been noticing by analyzing the results of MD simulations is that the bulk phase of these materials shows evidence for aggregation phenomena due to the formation of clusters made by like-charge ions (specifically anions). This evidence transforms the common concept that ILs can be thought as constituted by a disordered array of alternating

Received: July 11, 2018
Accepted: August 22, 2018
Published: September 5, 2018

DOI: 10.1021/acsomega.8b01615
ACS Omega 2018, 3, 10589−10600

charges. The existence of like-charge molecular interactions in ILs has already been noticed in other ILs,[28−32] where the presence of H-bond-driven, cationic complexes has been detected.[33]

In the series of compounds that we shall present here, the clustering seems to take place between anions where, as we shall see, the cooperative effect of hydrogen bonds is sufficient to overcome the Coulomb repulsion. Here, we try to unravel the basic physics behind this surprising organization pattern that we have already proven to exist for some of the cholinium amino acid-based PILs (e.g., ref 11).

2. RELATIVE STABILITY OF ANION−CATION COUPLES

The series of compounds made by choline and a deprotonated amino acid anion show a clear homogeneity at the microscopic level. One of the most striking results is that by computing the properties of the isolated, gas-phase anion−cation ionic couples, all of the resulting structures look very similar. We have already elucidated this result in ref 35, where we have analyzed the behavior and the stability trend of the ionic couples obtained with eight different amino acid anions. We found that the binding energies were almost constant along the series and between 102 and 106 kcal/mol. An exception was represented by [His] that had a lower binding energy of 93 kcal/mol. The binding pattern of the ionic couples was found to be very similar along the series of amino acids and due to a strong hydrogen bonding between the hydroxyl of the cation and the carboxylate of the anion. This homogeneity of behavior in the cation−anion interaction was further confirmed by bulk simulations where the average (atomic pair) radial distance between the two oxygens partaking in the H-bond was substantially constant throughout the series, and its value turned out to range between 2.68 and 2.74 Å.

Despite the homogeneity at the microscopic level, the bulk properties of the ensuing liquids are very different (see refs 14 and 34). Viscosities range from 1.6 Pa s for [Ala] to more than 20 Pa s for [Glu] and [Asp]. Conductivities vary by 2 orders of magnitude along the series, and some compounds were liquid only above 90 °C.

It is therefore clear that cooperative, many-body effects are extremely important in these compounds and that the understanding of their properties cannot rely on the description of the isolated ionic couples. In this study, we extend our previous works to other amino acids, and we try to find an explanation for the variety of behaviors spotted by the experimental bulk measurements. We begin by presenting the association enthalpies for the ionic couples (cation−anion) examined in this work. The data are reported in Table 1. In this table we present the results obtained with three different functionals: plain B3LYP, dispersion-corrected B3LYP (D3-B3LYP), and a quite accurate functional based on MP2 correlation (D3-B2PLYP). For each functional, the computation of the optimal geometry has been repeated in a polarizable continuum solvent model (PCM, see Section 6 for further details).

Binding enthalpies are very large in the gas phase where they substantially reproduce our old data of ref 35. The data obtained with D3-B3LYP and D3-B2PLYP are very similar with only a few tenths of kcal variation. It is worth noting that without dispersion correction these enthalpies turn out to be about 5−10 kcal less negative.

Table 1. $\Delta H°$ of the Cation−Anion Association in kcal/mol with the 6-311+G Basis Set[a]**

	B3LYP		B3LYP-D3		B2PLYP-D3	
	vacuo	PCM ε = 35.7	vacuo	PCM ε = 35.7	vacuo	PCM ε = 35.7
Ala	−97.5	−10.6	−102.8	−15.4	−102.3	−14.9
Val	−97.8	−10.6	−103.7	−15.7	−103.2	−15.1
Nva	−98.0	−10.6	−103.8	−15.4	−103.3	−14.9
Leu	−97.6	−10.7	−103.4	−15.3	−102.9	−14.8
Ile	−97.5	−10.4	−103.5	−15.5	−102.9	−14.9
Nle	−96.1	−9.6	−102.2	−14.7	−101.8	−14.4
Pro	−95.7	−10.2	−101.0	−15.1	−100.3	−14.5
Phe	−94.2	−10.6	−102.4	−16.7	−102.3[b]	−16.4[b]
Thr	−94.3	−10.1	−100.2	−14.9	−99.7	−14.3
His	−80.1	−7.3	−91.0	−13.5	−90.9	−13.3
Asp	−80.2	−7.1	−88.7	−12.0	−88.4	−11.6
Glu	−83.3	−2.1	−91.3	−6.8	−91.1	−6.5
Cys	−93.5	−10.1	−107.4	−14.7	−97.2	−14.3

[a]All data have been corrected for zero-point energy (ZPE) differences. [b]Obtained with 6-31+G**.

Obviously, these numbers are greatly reduced in a model continuum solvent because of the screening due to the presence of the dielectric and due to the solvation energies of the dissociated fragments. As we can see, the [His] and [Asp] and [Glu] ionic couples are the least bound among all.

All of the above ionic couples are characterized by essentially the same structure. Apart from the obvious electrostatic interaction, the general binding motif sees a strong H-bonding feature between the cation OH and the carboxylate O^-. The O−O distances are very similar along the series, ranging from 2.64 to 2.70 Å. We clearly see that the main binding features in the ionic couples are extremely homogeneous along the series and that the substantially different behavior of the resulting bulk phase must derive from collective effects.

3. RELATIVE STABILITY OF ANION−ANION AGGREGATES

One of the possible explanations for the different bulk behavior relies on the, rather obvious, assumption that it must derive from the anion structure that represents the "tunable" moiety in the fluid. As we have already pointed out in ref 11, we have discovered that the local microscopic structure of these liquids can be very complex. This complexity is due to a series of interrelated features:

- the amino acid anions can bind to each other through H-bonding features whose stability is much less than the cation−anion H-bond mentioned above but, nevertheless, can still be a relevant source of cohesive energy in the bulk;
- the anionic amino acid partner can undergo a tautomerization reaction and become an anionic zwitterion,[37] whose charge distribution is rather different from the plain anionic form; this tautomerization takes place for those amino acid anions that possess an additional, second protic function on the side chain (for example, another carboxyl or an −SH group), whose proton can be internally transferred to the amino group;
- amino acid anions, when interacting through H-bonds, can undergo intermolecular proton transfer, altering the local charge distribution of the bulk.

DOI: 10.1021/acsomega.8b01615
ACS Omega 2018, 3, 10589−10600

Table 2. $\Delta H°$ of the Anion−Anion Association in kcal/mol[a]

	B3LYP		B3LYP-D3		B2PLYP-D3		
	vacuo	ε = 35.7	vacuo	ε = 35.7	vacuo	ε = 35.7	ratio
Ala		1.8		−1.6		−1.1	0.07
Val		1.7		−2.2		−2.1	0.14
Nva		0.7		−3.1		−2.9	0.19
Leu		1.5		−3.5		−3.6	0.24
Ile		2.3		−2.2		−2.4	0.16
Nle		3.4		−2.8		−3.6	0.25
Pro		4.3		0.9		0.5	−0.03
Phe		1.6		−4.3		−4.7[b]	0.29
Thr	39.7	−1.1	36.8	−5.4	34.7	−5.5	0.38
His	34.3	3.5	28.5	−9.8	28.3[b]	−10.0[b]	0.75
Asp	39.6	1.7	37.5	−2.3	37.6	−2.4	0.21
Glu	31.6	−2.5	30.5	−3.9	30.7	−4.4	0.67
Cys	38.0	0.7	35.9	−3.8	36.4	−3.7	0.26

[a]All data have been corrected for ZPE. [b]Obtained with 6-31+G**. The last column on the right contains the ratio between the anion−anion B2PLYP/PCM binding energy and the anion−cation one of Table 1.

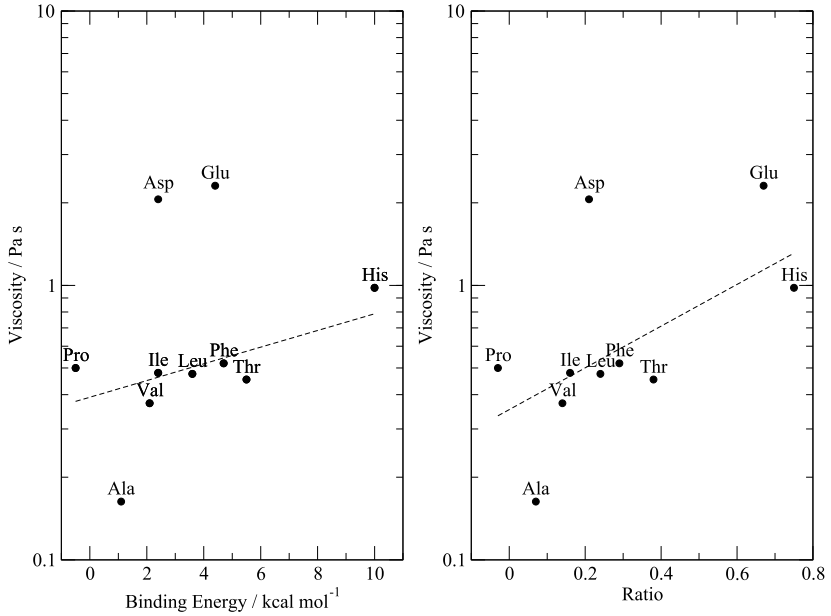

Figure 1. (Left) Anion−anion binding energies vs measured viscosity values for selected PILs. (Right) Ratio of the anion−anion and anion−cation binding energies vs measured viscosities. An exponential regression (dashed line) is also shown.

To quantify the importance of these phenomena, we have decided to evaluate the relative stability of the dimeric anionic clusters using ab initio techniques. This is by no means an obvious task, as the anionic pairs naturally tend to dissociate in vacuum. We have, therefore, performed the computations using a dielectric continuum solvent medium to screen the Coulomb repulsion and provide a more realistic modeling of the real bulk environment. Dielectric constants in PILs range from 20 to 80 depending on the number of electron-rich atoms in the molecular structures. We have exploited this fact and we have chosen a model solvent (acetonitrile) that has a dielectric constant of 35.7 that represents a value in line with available measurements, but that was not so high as to provide a testing ground only for highly oxygenated compounds.

The results obtained in a similar fashion to the ones presented for the cation−anion couples are in Table 2. Most of the amino acids do not show the presence of a minimum for the two interacting anions in the gas phase. It might sound surprising, but, despite the inherent instability of the gas-phase, like-charge dimers, we see that a few amino acids (specifically [Thr], [His], [Asp], [Glu], and [Cys]) were able to form metastable complexes, whose structures are actual high-energy minima on the potential energy surface, even without a dielectric (Table 2, first column). In particular, the [His] and [Glu] amino acid anions seem to be rather striking examples of the stability of such unlikely structures, providing a hint that anionic, like-charge clustering in these systems can be more common than one might surmise.

Almost all of the examined amino acid anion dimers (at the D3-B3LYP and D3-B2PLYP levels) are stable (of a few kcal) with respect to dissociation when immersed in a sufficiently screening dielectric. Only for [Pro] have we been unable to find a structure with a negative association energy. For all compounds, dispersion forces do play a crucial role in allowing the stabilization of such elusive complexes.

DOI: 10.1021/acsomega.8b01615
ACS Omega 2018, 3, 10589−10600

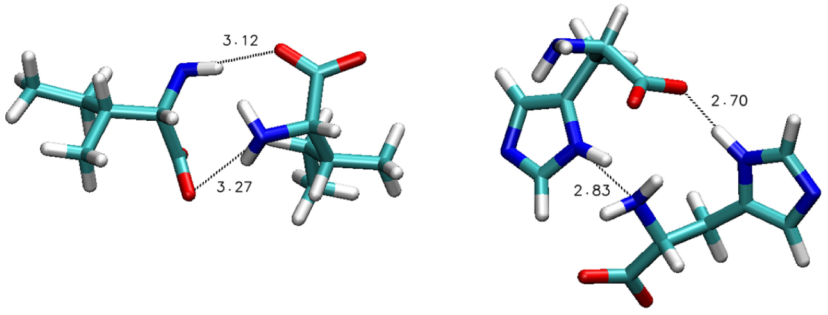

(a) [Ile] (b) [His]

Figure 2. Optimized structures at the D3-B3LYP/PCM level for [Ile] (a) and [His] (b) anionic dimers. Acceptor−donor distances in H-bonds are also shown.

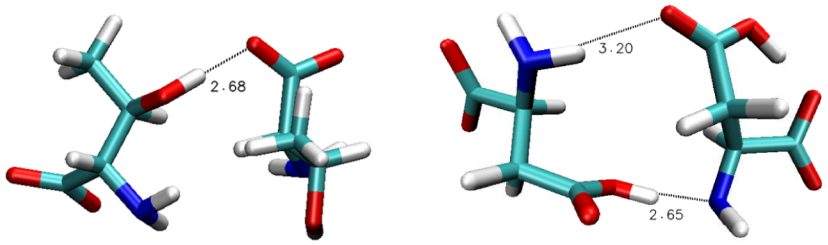

(a) [Thr] (b) [Asp]

Figure 3. Optimized structures at the D3-B3LYP/PCM level for [Thr] (a) and [Asp] (b) anionic dimers. Acceptor−donor distances in H-bonds are also shown.

As we can see from Table 2, a particularly large stabilization energy is obtained for [His], [Thr], and [Glu], where the anion−anion binding energy turns out to be a substantial amount of the anion−cation one (last column in Table 2). For all other amino acid anions, the anion−anion binding energy is significantly smaller than the cation−anion one, even though for some systems the former could account for one-fourth of the total cohesive energy.

As anion−anion dimers seem to be likely to occur, we can assume that it is precisely this additional cohesive mechanism that differentiates the bulk behavior along the series. To strengthen this conclusion, we show in Figure 1 (left panel) a plot in which we have reported the anion−anion binding energies as determined by us (x-axis) and the experimental viscosities (y-axis). There is a correlation between the binding energy of the dianions and the bulk friction for most of the amino acids (beware that the relation between viscosity and energy is logarithmic), whereas the [Asp], [Glu], and [Ala] cases seem to provide an interesting exception. In Figure 1, we have also reported the same viscosity data as a function of the "ratio" column of Table 2, i.e., the ratio between the anion−anion binding energy and the cation−anion one. In this case, we see a better correlation between the relative importance of the anion−anion cohesive energy and a greater friction in the fluid. Although the fact that the ability of a component of the fluid to establish H-bonds provides additional friction might sound as an obvious statement, much less obvious is the fact that the additional cohesive energy might come from like-charge clustering.

The stabilization of these anion−anion structures is due mainly to H-bonding features, depending on the side chain nature and functional groups. As a first example, we report in Figure 2a the optimized structures of the [Ile] dimer, which is representative of the amino acids with an aliphatic side chain. Aliphatic amino acid anions bind each other via two weak H-bonds, whose acceptor−donor distances are larger than 3 Å. These H-bonding features come in pairs, except for [Nle] for which we have found a low-energy structure with only one H-bond. The connections are established between the carboxylate and the amino group. As is obvious, such a double H-bond arrangement can exist in the liquid only if the carboxylate function is not already bound to the choline hydroxyl. Therefore, we deem that such H-bonds are only seldom formed in the bulk liquid, although it is certainly possible that an arrangement with a single H-bond may exist as a transient feature owing to the bidentate nature of the carboxylate group.

The [His] compound (shown in Figure 2b) is a more interesting case, where one of the H-bonds between anions is established between the aliphatic amino group and the imidazole ring, therefore without requiring the intervention of a carboxylate. Such an H-bond in our optimized structure has an acceptor−donor distance of 2.83 Å, which points to a stronger binding with respect to what we have seen for the aliphatic amino acids. As we see in Table 2, the binding energy between two anions in their most favorable geometry amounts to 75% of the anion−cation binding energy. This makes the [His][Ch] IL certainly an interesting case, where anionic clustering can be an additional source of cohesive energy that can represent the reason for its high viscosity.

The [Thr] anion (Figure 3a) has a hydroxyl group at the end of the side chain that binds strongly to one of the carboxylate oxygens. Its binding energy is, however, rather small and comparable to other aliphatic or aromatic side chains (e.g., [Phe]). Nevertheless, the peculiar presence of the hydroxyl, as we shall see later, provides a bulk nanostructure which is quite unique in the series.

DOI: 10.1021/acsomega.8b01615
ACS Omega 2018, 3, 10589−10600

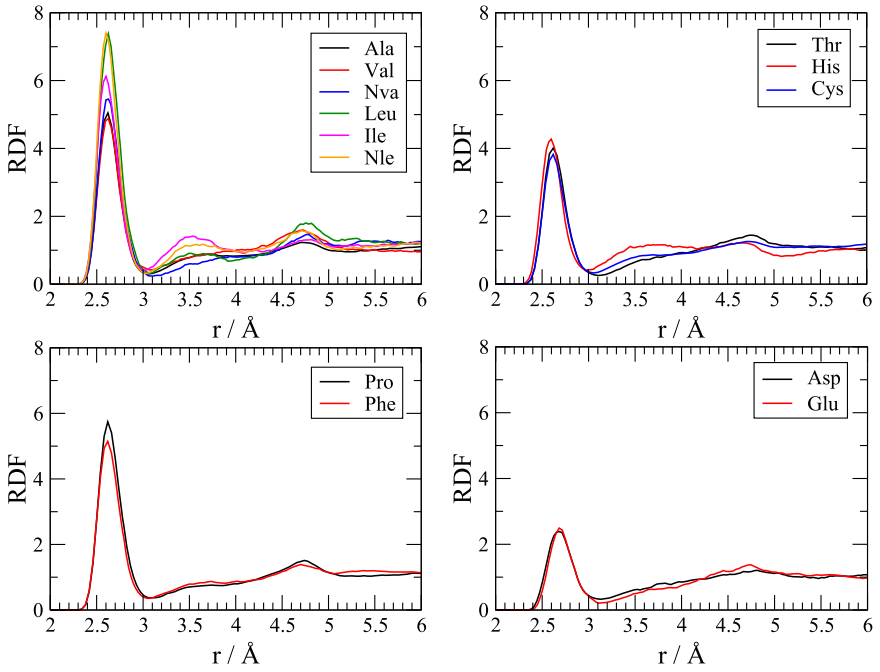

Figure 4. Cation−anion oxygen−oxygen RDFs from AIMD bulk simulations of several amino acid liquids. The atoms involved are the oxygen of the hydroxyl on choline and the oxygen on the (deprotonated) carboxylate of the amino acid.

The [Asp] and [Glu] cases are similar to each other (see Figure 3b). These anions bind through a "salt-bridge" double bond, which is known to be particularly stable, hence the rather high binding energy that is a significant fraction of the anion−cation one. At difference with previous cases, the anion−anion binding pattern involves only non-negatively charged functional groups. The two negative carboxylates point outside the dimer to minimize their Coulomb repulsive interaction. These geometrical features, as we shall see below, indicate that the structure of the corresponding liquids cannot be that of an alternating pattern of anions and cations but is certainly more complex with a high degree of anionic association.

4. CONNECTION WITH BULK SHORT-RANGE STRUCTURE

All of the above ILs have been simulated in their bulk state by us using AIMD in the past few years (e.g., see ref 12 and the Supporting Information, Table S1 for further details on the simulation protocols). Different paradigms and different functionals have been used, and therefore, we should compare the results with caution. Nevertheless, many of the simulations have been carefully validated using experimental structural and spectroscopic data, and we believe that the quality of the computations is sufficient to interpret the bulk nanoscopic structure (e.g., see refs10−12). Finally, we remark that all data extracted from the bulk simulations come from calculations where the forces have been evaluated through ab initio density functional theory (DFT) computations of the electronic structure. Despite few well-known shortcomings of the DFT method, it is generally accepted that molecular dynamics simulations based on such ab initio paradigm are quite accurate in reproducing the short-range structure of the fluid and generally, in this respect, show a superior accuracy compared to force field-based approaches.

We begin by reporting the radial distribution function (RDF in the following) of the O−O pairs involved in the cation−anion ionic couples, as extracted by the AIMD bulk simulations. As we have shown above, the anion−cation O−O H-bond is, apart from being electrostatic, the main structuring feature of the bulk fluids. The data are reported in Figure 4 and their purpose is to show, once again, how the anion−cation binding motif is the same along the series of amino acid liquids. The average O−O distance is substantially a constant throughout the amino acid series with a small difference for [Asp] and [Glu], where it turns out to be slightly larger, indicating a somewhat reduced interaction (in accord with the data of Table 1). In Table 3, the O−O RDF maximum distances are compared to those obtained from the ab initio optimization of the anion−cation pair seen above.

Table 3. Anion−Cation O−O Distuted by Ab Initio Optimization (Ab Initio) on a Single Ionic Couple (D3-B3LYP/PCM Level) and O−O Average Distances as Extracted from AIMD Simulations (MD)

res.	r_{O-O} (ab initio)	r_{O-O} (MD)
Ala	2.65	2.62
Val	2.67	2.62
Nva	2.66	2.63
Leu	2.66	2.62
Ile	2.67	2.60
Nle	2.67	2.60
Pro	2.65	2.62
Phe	2.64	2.62
Thr	2.67	2.62
His	2.71	2.60
Asp	2.70	2.68
Glu	2.66	2.68
Cys	2.66	2.62

DOI: 10.1021/acsomega.8b01615
ACS Omega 2018, 3, 10589−10600

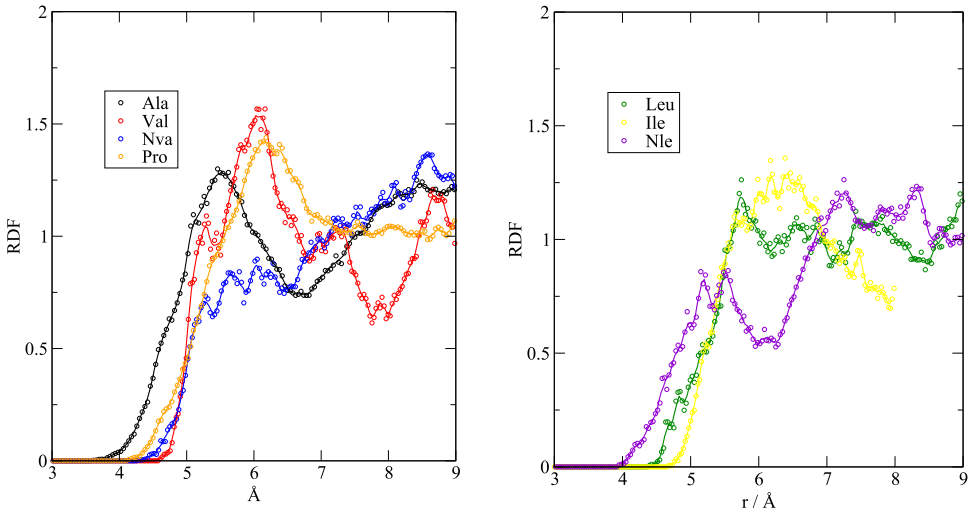

Figure 5. Anion−anion center-of-mass RDFs as extracted from bulk simulations for several amino acid-based liquids.

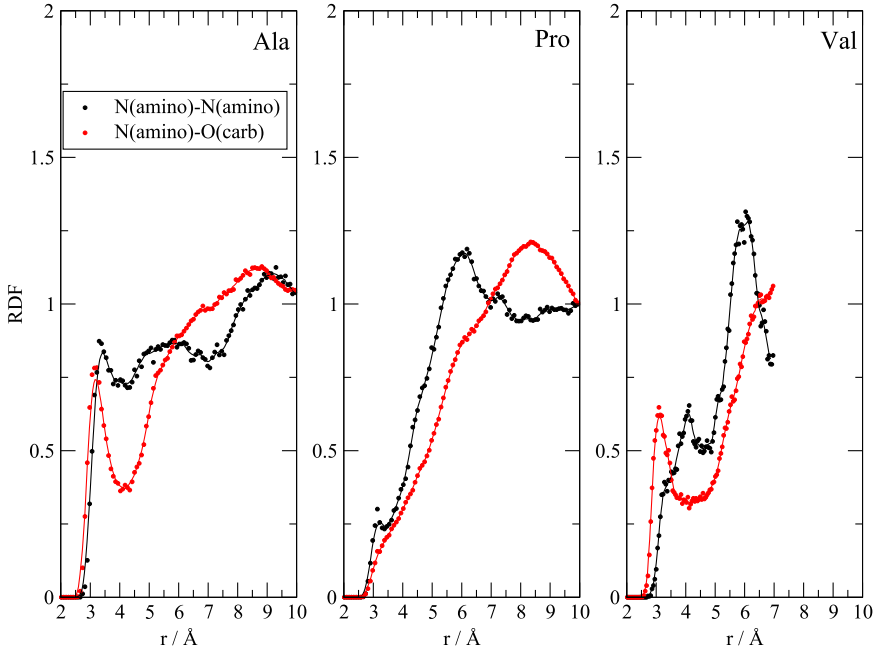

Figure 6. N−N and N−O interanionic RDFs for [Ala] (left), [Pro] (center), and [Val], right.

By looking at these data alone, the great difference in internal friction and viscosities is completely unexplained. The reduced interaction in the [Glu] and [Asp] ionic couples should even point to a reduced friction in these systems which, instead, show the highest viscosities and the highest melting temperatures.[14] The differentiation in bulk properties should therefore arise from somewhere else.

To understand the extent to which anion−anion interactions can play a role in this additional stabilization, we shall discuss in the following the RDF between the anionic centers-of-mass as extracted from the molecular dynamics simulations. These RDFs are a rough measure of how far the anions find themselves in the liquid with respect to each other. We begin by showing in Figure 5 the anion−anion RDF for the amino acids with an aliphatic side chain. As we are dealing with bulky anions, all distances are large, but we can clearly see that in the case of [Val], the RDF shows a profile with a peak just above 5 Å. This peak exists also, albeit to a lesser extent, for [Nva] and [Nle]. [Pro], [Ile], and [Leu], instead, have a RDF profile that seems to imply a purely repulsive interaction between anions. [Ala] represents a kind of special case, where the presence of anion−anion distances below 5 Å might be a peculiar consequence of its small size. To further elucidate the situation, we can safely assume that the only possible interanionic contact comes from H-bonds between two amino groups or between an amino group and a carboxylate. We report in Figure 6 the N−N and N−O RDFs between the anions for three different amino acid representatives of the behavior seen above. The sharp peak at about 3 Å (red line) in [Val] and [Ala] points to the presence of a N−O (amino-carboxylate) H-bond, which in turn shows that anions (even in the case of the less bulky [Ala] compound) can interact directly without the mediation of a cation. In these two liquids, the amino group shows hints of an interaction with the same group of another anion (black curves/points). [Pro][Ch], on the other hand, does not show such interactions in accord with

DOI: 10.1021/acsomega.8b01615
ACS Omega 2018, 3, 10589−10600

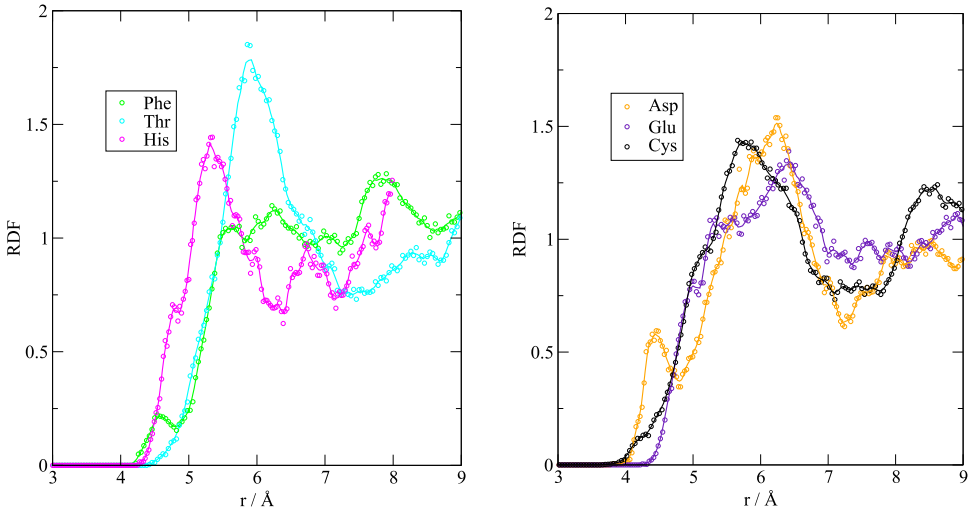

Figure 7. Anion−anion center-of-mass RDFs as extracted from bulk simulations for several amino acid-based liquids.

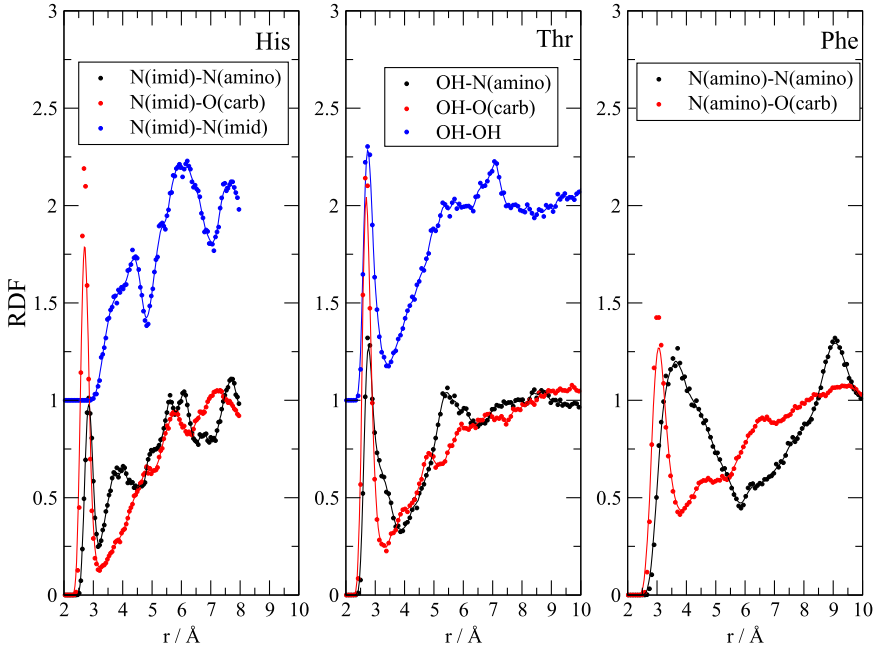

Figure 8. N−N and N−O interanionic RDFs for [His] (left) and [Phe] (right). For [Thr] (middle panel), the data pertaining to the side chain hydroxyl are also shown.

the positive anion−anion binding energy reported in Table 2. The viscosity of the [Pro][Ch] liquid with respect to [Ala][Ch], therefore, seems to be due to other mechanisms of interactions, probably involving dispersion forces.

A second set of anion−anion RDF is reported in Figure 7, where we can see the behavior of the amino acid with nonaliphatic side chains. A compact arrangement of anions can be noted for [His], where the average anion−anion distance is only slightly above 5 Å, as in [Ala], despite the much bigger size of the molecular ions. The anionic clustering in these fluids takes place via H-bond formation, as in the previous cases. In particular, in Figure 8 (on the left), we show the [His] interanionic N−O and N−N RDFs, where we see the clear imprints of the presence of interanionic interactions between the imidazole group and the heteroatoms of another anion. For [His], the interaction is mainly with the carboxylate (red curve/dots), where the acceptor−donor distance is 2.6 Å, thereby pointing to a rather strong H-bond. This interanionic coupling mechanism between the ionic moieties in the [His][Ch] fluid can be easily put in relation with the high viscosity of the liquid, as shown in Figure 1. It is interesting to note that the H-bond donor ability of the imidazole NH group is almost completely expressed toward the carboxylate, whereas the N−N H-bonding between two imidazoles (blue dots) is suppressed. An example of the anionic aggregation of two [His] anions is provided in Figure 9 using a dimer as extracted from one frame of our AIMD simulation.

In the middle panel of Figure 8, we report a set of data pertaining to the [Ch][Thr] liquid, where the additional hydroxyl on the side chain allows for a total of three different H-bonding features between anions. The hydroxyl groups can establish connections toward the amino group (black), the carboxylate (red), and among themselves (blue). Also in the [Thr] case, all of these H-bonds are quite strong with an

DOI: 10.1021/acsomega.8b01615
ACS Omega 2018, 3, 10589−10600

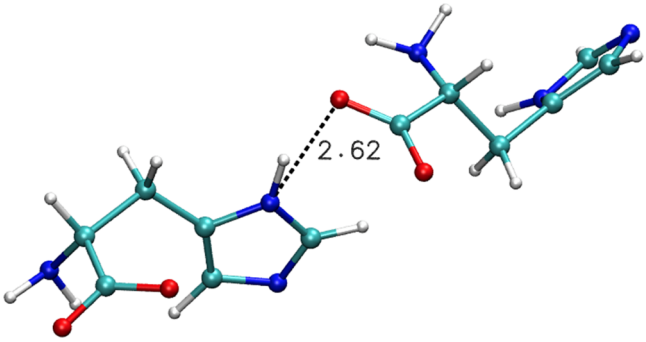

Figure 9. Example of one of the ionic dimers occurring in the [His][Ch] liquid simulation connected through an imidazole−carboxylate H-bond.

acceptor−donor distance ranging from of 2.6−2.8 Å. This network of H-bonds gives rise to a very complex structure where chains of molecular anions are bound together. The peculiar structure of [Thr][Ch] is shown pictorially in Figure 10 by means of a surface representation of three snapshots of the simulation box taken at different times. The surface enclosing the anions (red) clearly shows aggregation phenomena on the nanoscopic scale, whereas the surface enclosing cations (blue) show that almost all molecular cations are isolated from each other.

The [Phe][Ch] liquid (Figure 8, right panel), instead, provides an example where both N−N and the N−O interanionic H-bonds play a role, albeit the latter is predominant in strength and coordination ability, as shown by the sharpness of the relative peak (red dots in Figure 8).

To conclude this section, we now move to the analysis of the last group of amino acid anions, i.e., those reported in the right panel of Figure 7. [Cys], [Asp], and [Glu] possess an additional acidic function on the side chain (whose acidity in terms of pK_a's is very weak for [Cys], weak for [Asp] and [Glu]). The structure of these compounds is therefore complicated by the fact that the proton on these acidic functions is not stable but can move to other anions.[37]

In [Cys][Ch], the main anionic aggregation is due to a weak (and quite elongated) S−S interaction, as shown in Figure 11 where we also see that the S−O and S−N interactions have only a limited extent in the fluid. This S−S interaction coupled to the one between amino groups and carboxylates (right panel in Figure 11) induces the presence of large anionic aggregates. Within these aggregates, proton transfer is possible, as shown by the two snapshots reported in Figure 12, where two of the S−H protons have moved onto a nearby amino group (one within the same molecule). The proton transfers have created two positively charged $-NH_3^+$ groups, whose H-bond has shortened increasing its strength.

Finally, we observe the peculiar structure of the liquids containing [Asp] and [Glu]. They are similar in properties, as they both have an acidic proton on the side chain. Both compounds are very viscous even at 80 °C,[14] and both have high melting points. In the simulations, we have implicitly assumed that only one of the carboxylate protons has been removed because a complete deprotonation leads to solid compounds.[14]

The elusive proton transfer noted in the [Cys] case, here turns out to be an important chemical process that alters the structure and dielectric properties of the bulk. From the point of view of a short-range structure, we see in Figure 13 that the [Asp] anions (left panel) are in contact through mainly H-bonds that involve the OH (on the nondeprotonated side chain) and the carboxylate of the amino group (compare also Figure 3). It turns out that N−N and the O(carboxylate)−N contacts are much less important. A density representation of the AIMD trajectory (reported in Figure 14) clearly shows the nanoscopic anionic organization (in red) and the corresponding lack of cation−cation interactions in much the same way we have already found for the [Thr]-based liquid. An example of a cluster of anions is also reported in Figure 14. In the [Glu] liquid, the situation is not completely dissimilar, but we have

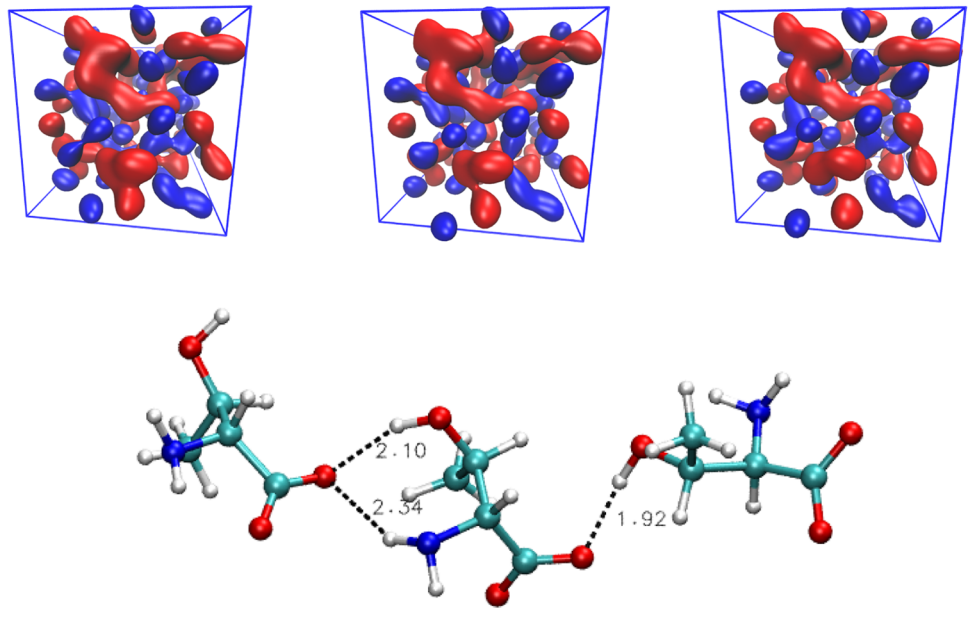

Figure 10. (Top) Surface representation of the bulk liquid [Thr][Ch] as obtained by three snapshots of the AIMD simulation: anion density in red, cation density in blue. (Bottom) One of the anionic trimers identified in the simulation box with its H-bonds.

DOI: 10.1021/acsomega.8b01615
ACS Omega 2018, 3, 10589−10600

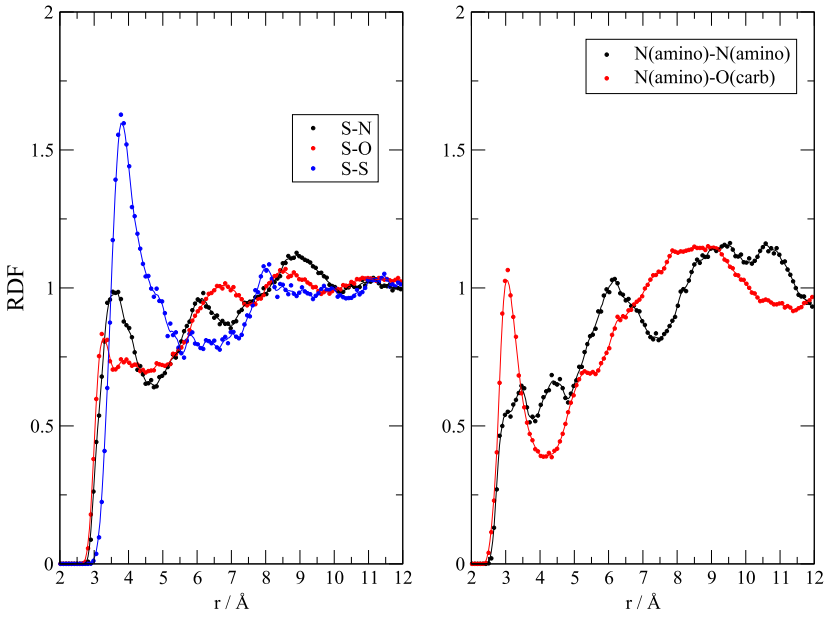

Figure 11. [Cys][Ch] interanionic RDFs.

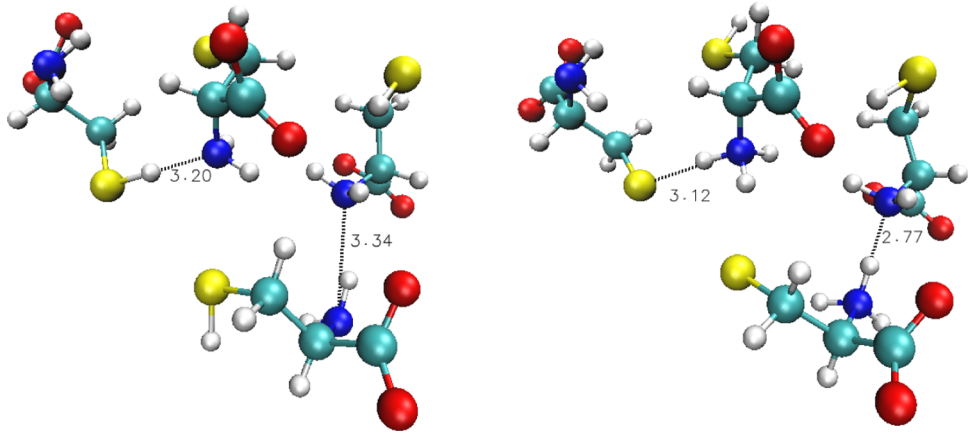

Figure 12. Anionic clustering in [Cys][Ch]: two snapshots of an anionic cluster (four [Cys] anions) as detected in the AIMD simulation, where all other molecules have been removed from the representation for clarity. Two proton transfers have taken place between the two snapshots in going from left to right (one intermolecular and one intramolecular).

found that the presence of H-bonds between OH and the amino group is reduced.

5. CONCLUSIONS

The aim of this work is to describe from a general point of view the microscopic structure of complex ILs using a homologous series of compounds. Although most of the traditional, aprotic ionic liquids are characterized by a local structure that resembles a dynamical version of a crystalline salt, the existence of hydrogen bonds makes a PIL a more complex environment. It was rather surprising that a set of ILs, all synthesized using the same cation and slight variation of a substituent on the anion (the amino acid side chain), provided a remarkable variety of bulk behaviors in terms of fluid states and frictional properties. Obviously, this huge difference in the bulk state/properties had to come from the variation of the anionic molecular constituents.

In particular, we have seen (and reported here) that the main binding motif between anions and cations is rather similar for all different amino acids involved. This motif involves a strong OH−O hydrogen bond between the cation hydroxyl and the negatively charged carboxylate on the anions. The anion−cation dimer binding energies are almost the same for all amino acids, thereby leading us to conclude that the above differences must stem from somewhere else.

In the last few years we have been accumulating evidence that the PILs under investigations might present an unusual behavior in many respects: (i) amino acid anions do interact through hydrogen bonds; (i) these anions can undergo tautomerization, as neutral amino acid molecules do, creating a sort of anionic−zwitterionic molecular species; (ii) amino acid anions when interacting may also undergo intermolecular proton transfer. We have, therefore, devoted this work to the quantification and description of the interanionic interactions. This has been achieved by means of an accurate evaluation of the binding energies of the anionic dimers and through a novel analysis of several MD simulations, which we had performed (and sometimes already illustrated) previously. We have presented computational evidence that the frictional properties of this class of liquids could be linked to their ability to form

DOI: 10.1021/acsomega.8b01615
ACS Omega 2018, 3, 10589−10600

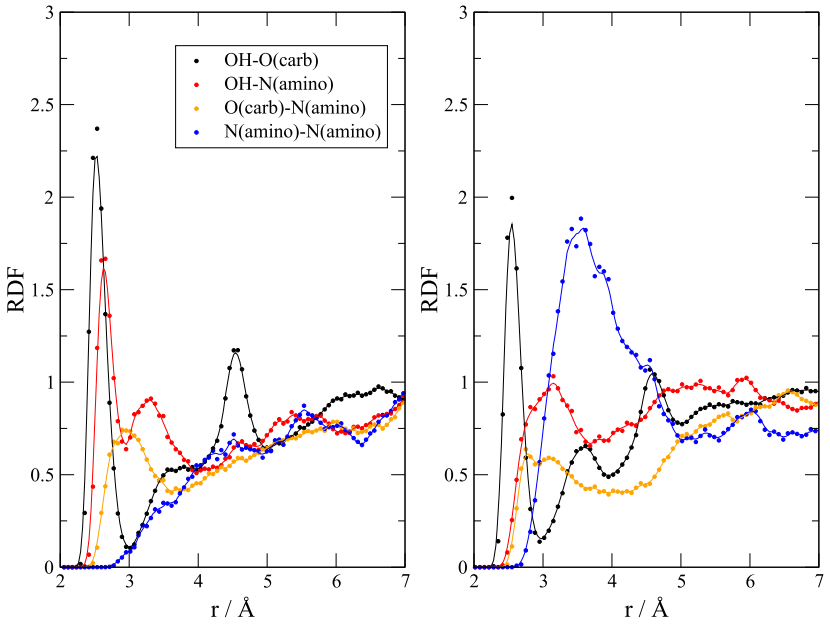

Figure 13. Interanionic RDFs for [Glu][Ch] (right) and [Asp][Ch] (left).

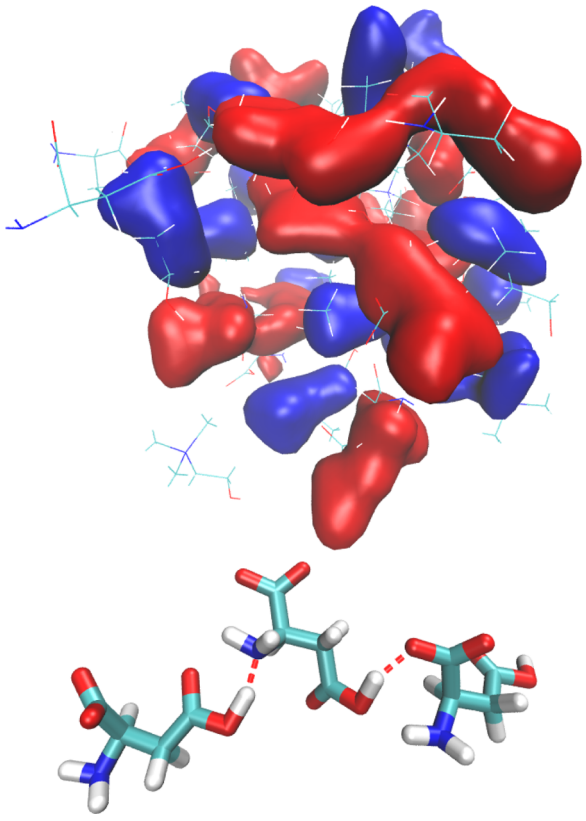

Figure 14. (Top) Density surface representation of the bulk liquid [Asp][Ch] as obtained by a positional average of the AIMD snapshots: anion density in red, cation density in blue. (Bottom) One of the anionic trimers identified in the simulation box with its H-bonds.

additional H-bonding features. We have also shown that, remarkably, these H-bonding features tend to cluster the anionic moieties, giving rise to a variety of interanionic interactions, whose strength and properties depend strongly on the side chain chemical properties. It, therefore, follows that one must be aware of the existence of strong interanionic interactions when dealing with such fluids (or at least a subset of them) and that an understanding of their local structure cannot be simply obtained by ionic couple modeling or other over-simplified (two-body) models. In addition, we suggest that the interpretation of anomalous or unexpected experimental data pertaining to this class of materials should not be conducted under the assumption that the ionic moieties live in separated domains but that the spatial contiguity of interacting anions could provide the driving forces for the formation of a nonobvious structural and chemical organization.

6. COMPUTATIONAL METHODS

Ab initio static calculations have been performed on the isolated (anion−cation) ionic couples made by an amino acid anion (13 variants) and a choline cation (see ref 35 for analogous computations) and on the anionic dimer made by 2 identical deprotonated amino acids. For each combination, the calculations have been performed both in the gas phase and in a polarizable continuum solvent model (PCM). As the dielectric permittivity of these compounds has not been reported in the literature so far, acetonitrile has been employed as a model solvent, given that its dielectric constant has the typical value of PILs.[36] We have shown previously[37] that the actual value of the dielectric constant is a rather insensitive parameter, given that the relative stability of the amino acid anion isomers does not appear to change upon its significant variation in a rather large range from 20 to 80. For each dimer, we have optimized the structure and evaluated the harmonic frequencies using three functionals: B3LYP, D3-B3LYP,[38] and D3-B2PLYP[39] all with the 6-311+G** basis set (except for [Phe] where the smaller 6-31+G** was used to perform the rather intensive B2PLYP frequency computations). The Gaussian16[40] package has been used for all calculations. The 13 amino acid structures and their conventional names are reported in Figure S1.

Several papers by us[10−12] have appeared recently in the literature where we have presented AIMD results on various compounds. These data will be used in this paper as an

DOI: 10.1021/acsomega.8b01615
ACS Omega 2018, 3, 10589−10600

additional source of information that allows drawing a connection between the static calculations and the bulk phase. The AIMD bulk simulation on the [Glu][Ch] anion, which have not been presented before, has been done using the Car−Parrinello molecular dynamic[41] code using a cell with a side length of 20.5 Å containing 24 ionic pairs. Car−Parrinello molecular dynamics has been performed employing the BLYP functional and Troullier−Martins[42] pseudopotentials. The production time was 33 ps at 300 K with a constant density of 1.14 gr/cm^3. For comparison, the simulation parameters and protocols of all other systems are reported in Table S1.

■ ASSOCIATED CONTENT

Supporting Information

The Supporting Information is available free of charge on the ACS Publications website at DOI: 10.1021/acsomega.8b01615.

Structural formulae of the amino acids mentioned in this paper (Figure S1); ab initio optimized structures of all amino acid anionic pairs, as obtained from the B3LYP/6-311+G**/PCM method (Figure S2); simulation data for all bulk simulations (cell lengths, densities, functional for the forces, time-span, temperature) (Table S1) (PDF)

■ AUTHOR INFORMATION

Corresponding Author

*E-mail: enrico.bodo@uniroma1.it.

ORCID

Enrico Bodo: 0000-0001-8449-4711

Notes

The authors declare no competing financial interest.

■ ACKNOWLEDGMENTS

Financial support from "La Sapienza" (grant no. RM116154CA141A23) is acknowledged. E.B. and A.L.D. gratefully acknowledge the computational support of CINECA (grant IscrC_AAAOX) and PRACE (grant no. 2016163881).

■ REFERENCES

(1) Greaves, T. L.; Drummond, C. J. Protic ionic liquids: evolving structure−property relationships and expanding applications. *Chem. Rev.* **2015**, *115*, 11379−11448.

(2) Bodo, E.; Sferrazza, A.; Caminiti, R.; Mangialardo, S.; Postorino, P. A prototypical ionic liquid explored by ab initio molecular dynamics and Raman spectroscopy. *J. Chem. Phys.* **2013**, *139*, No. 144309.

(3) Belieres, J.-P.; Angell, C. A. Protic ionic liquids: preparation, characterization, and proton free energy level representation-. *J. Phys. Chem. B* **2007**, *111*, 4926−4937.

(4) Greaves, T. L.; Ha, K.; Muir, B. W.; Howard, S. C.; Weerawardena, A.; Kirby, N.; Drummond, C. J. Protic ionic liquids (PILs) nanostructure and physico chemical properties: development of high-throughput methodology for PIL creation and property screens. *Phys. Chem. Chem. Phys.* **2015**, *17*, 2357.

(5) Doi, H.; Song, X.; Minofar, B.; Kanzaki, R.; Takamuku, T.; Umebayashi, Y. A new proton conductive liquid with no ions: pseudo-protic ionic liquids. *Chem. - Eur. J.* **2013**, *19*, 11522−11526.

(6) Stoimenovski, J.; Izgorodina, E. I.; MacFarlane, D. R. Ionicity and proton transfer in protic ionic liquids. *Phys. Chem. Chem. Phys.* **2010**, *12*, 10341−10347.

(7) Bodo, E.; Mangialardo, S.; Capitani, F.; Gontrani, L.; Leonelli, F.; Postorino, P. Interaction of a long alkyl chain protic ionic liquid and water. *J. Chem. Phys.* **2014**, *140*, No. 204503.

(8) Campetella, M.; Gontrani, L.; Leonelli, F.; Bencivenni, L.; Caminiti, R. Two different models to predict ionic-liquid diffraction patterns: fixed-charge versus polarizable potentials. *Chem. Phys. Chem.* **2015**, *16*, 197−203.

(9) Fumino, K.; Fossog, V.; Stange, P.; Paschek, D.; Hempelmann, R.; Ludwig, R. Controlling the subtle energy balance in protic ionic liquids: dispersion forces compete with hydrogen bonds. *Angew. Chem., Int. Ed.* **2015**, *54*, 2792−2795.

(10) Campetella, M.; Montagna, M.; Gontrani, L.; Scarpellini, E.; Bodo, E. Unexpected proton mobility in the bulk phase of cholinium-based ionic liquids. new insights from theoretical calculations. *Phys. Chem. Chem. Phys.* **2017**, *19*, 11869−11880.

(11) Campetella, M.; Le Donne, A.; Daniele, M.; Gontrani, L.; Lupi, S.; Bodo, E.; Leonelli, F. Hydrogen bonding features in cholinium-based protic ionic liquids from molecular dynamics simulations. *J. Phys. Chem. B* **2018**, *122*, 2635−2645.

(12) Campetella, M.; Bodo, E.; Montagna, M.; De Santis, S.; Gontrani, L. Theoretical study of ionic liquids based on the cholinium cation. Ab initio simulations of their condensed phases. *J. Chem. Phys.* **2016**, *144*, No. 104504.

(13) Usula, M.; Matteoli, E.; Leonelli, F.; Mocci, F.; Marincola, F. C.; Gontrani, L.; Porcedda, S. Thermo-physical properties of ammonium-based ionic liquid + N-methyl-2-pyrrolidone mixtures at 298.15 K. *Fluid Phase Equilib.* **2014**, *383*, 49−54.

(14) Masci, G.; De Santis, S.; Casciotta, F.; Caminiti, R.; Scarpellini, E.; Campetella, M.; Gontrani, L. Cholinium amino acid based ionic liquids: a new method of synthesis and physico-chemical characterization. *Phys. Chem. Chem. Phys.* **2015**, *17*, 20687−20698.

(15) Hou, X.-D.; Liu, Q. P.; Smith, T. J.; Li, N.; Zong, M. H. Evaluation of toxicity and biodegradability of cholinium amino acids ionic liquids. *PLoS One* **2013**, *8*, No. e59145.

(16) Weaver, K. D.; Kim, H. J.; Sun, J.; MacFarlane, D. R.; Elliott, G. D. Cyto-toxicity and biocompatibility of a family of choline phosphate ionic liquids designed for pharmaceutical applications. *Green Chem.* **2010**, *12*, 507−513.

(17) Nockemann, P.; Thijs, B.; Driesen, K.; Janssen, C. R.; Van Hecke, K.; Van Meervelt, L.; Kossmann, S.; Kirchner, B.; Binnemans, K. Choline saccharinate and choline acesulfamate: ionic liquids with low toxicities. *J. Phys. Chem. B* **2007**, *111*, 5254−5263.

(18) Stoimenovski, J.; Dean, P. M.; Izgorodina, E. I.; MacFarlane, D. R. Protic pharmaceutical ionic liquids and solids: aspects of protonics. *Faraday Discuss.* **2012**, *154*, 335−352.

(19) Hough, W. L.; Smiglak, M.; Rodríguez, H.; Swatloski, R. P.; Spear, S. K.; Daly, D. Y.; Pernak, J.; Grisel, J. E.; Carliss, R. D.; Soutullo, M. D.; et al. The third evolution of ionic liquids: active pharmaceutical ingredients. *New J. Chem.* **2007**, *31*, 1429−1436.

(20) Fukaya, Y.; Iizuka, Y.; Sekikawa, K.; Ohno, H. Bio ionic liquids: room temperature ionic liquids composed wholly of biomaterials. *Green Chem.* **2007**, *9*, 1155−1157.

(21) Plaquevent, J.-C.; Levillain, J.; Guillen, F.; Malhiac, C.; Gaumont, A. C. Ionic liquids: new targets and media for amino acid and peptide chemistry. *Chem. Rev.* **2008**, *108*, 5035−5060.

(22) Petkovic, M.; Ferguson, J. L.; Gunaratne, H. Q. N.; Ferreira, R.; Leitao, M. C.; Seddon, K. R.; Rebelo, L. P. N.; Pereira, C. S. Novel biocompatible cholinium-based ionic liquids-toxicity and biodegradability. *Green Chem.* **2010**, *12*, 643−649.

(23) Tao, G. H.; He, L.; Liu, W. S.; Xu, L.; Xiong, W.; Wang, T.; Kou, Y. Preparation, characterization and application of amino acid-based green ionic liquids. *Green Chem.* **2006**, *8*, 639−646.

(24) Matsuoka, H.; Nakamoto, H.; Susan, M. A. B. H.; Watanabe, M. Brønsted acid base and poly base complexes as electrolytes for fuel cells under non-humidifying conditions. *Electrochim. Acta* **2005**, *50*, 4015−4021.

(25) Nakamoto, H.; Watanabe, M. Brønsted Acid-Base ionic liquids for fuel cell electrolytes. *Chem. Commun.* **2007**, 2539−2541.

(26) Timperman, L.; Skowron, P.; Boisset, A.; Galiano, H.; Lemordant, D.; Frackowiak, E.; Beguin, F.; Anouti, M. Triethylammonium bis(tetrafluoromethylsulfonyl)amide protic ionic liquid as an

DOI: 10.1021/acsomega.8b01615
ACS Omega 2018, 3, 10589−10600

electrolyte for electrical double-layer capacitors. *Phys. Chem. Chem. Phys.* **2012**, *14*, 8199−8207.
(27) Menne, S.; Pires, J.; Anouti, M.; Balducci, A. Protic ionic liquids as electrolytes for lithium-ion batteries. *Electrochem. Commun.* **2013**, *31*, 39−41.
(28) Knorr, A.; Stange, P.; Fumino, K.; Weinhold, F.; Ludwig, F. Spectroscopic evidence for clusters of like-charged ions in ionic liquids stabilized by cooperative hydrogen bonding. *ChemPhysChem* **2016**, *17*, 458−462.
(29) Strate, A.; Niemann, T.; Ludwig, R. Controlling the kinetic and thermodynamic stability of cationic clusters by the addition of molecules or counterions. *Phys. Chem. Chem. Phys.* **2017**, *19*, 18854.
(30) Strate, A.; Overbeck, V.; Lehde, V.; Neumann, J.; Bonsa, A.-M.; Niemann, T.; Paschek, D.; Michalik, D.; Ludwig, R. The influence of like-charge attraction on the structure and dynamics of ionic liquids: NMR chemical shifts, quadrupole coupling constants, rotational correlation times and failure of Stokes−Einstein−Debye. *Phys. Chem. Chem. Phys.* **2018**, *20*, 5617.
(31) Menges, F. S.; Zeng, H.; Kelleher, P.; Gorlova, O.; Johnson, M.; Niemann, T.; Strate, A.; Ludwig, R. Structural Motifs in Cold Ternary Ion Complexes of Hydroxyl-Functionalized Ionic Liquids: Isolating the Role of Cation-Cation Interactions. *J. Phys. Chem. Lett.* **2018**, *9*, 2979−2984.
(32) Niemann, T.; Stange, P.; Strate, A.; Ludwig, R. Like-likes-Like: Cooperative hydrogen bonding overcomes Coulomb repulsion in cationic clusters with net charges up to Q=+6e. *ChemPhysChem* **2018**, *19*, 1691−1695.
(33) Knorr, A.; Fumino, K.; Bonsa, A.-M.; Ludwig, R. Spectroscopic evidence of 'jumping and pecking' of cholinium and H-bond enhanced cation−cation interaction in ionic liquids. *Phys. Chem. Chem. Phys.* **2015**, *17*, 30978−30982.
(34) Liu, Q.-P.; Hou, X.-D.; Li, N.; Zong, M.-H. Ionic liquids from renewable biomaterials: synthesis, characterization and application in the pretreatment of biomass. *Green Chem.* **2012**, *14*, 304−307.
(35) Benedetto, A.; Bodo, E.; Gontrani, L.; Ballone, P.; Caminiti, R. Amino acid anions in organic ionic compounds. An ab-initio study of selected ion pairs. *J. Phys. Chem. B* **2014**, *118*, 2471.
(36) Huang, M.-M.; Jiang, Y.; Sasisanker, P.; Driver, G. W.; Weingartner, H. Static Relative Dielectric Permittivities of Ionic Liquids at 25 °C. *J. Chem. Eng. Data* **2011**, *56*, 1494−1499.
(37) Bodo, E.; Le Donne, A. Isomerization patterns and proton transfer in ionic liquids constituents as probed by ab-initio computation. *J. Mol. Liq.* **2018**, *249*, 1075−1082.
(38) Grimme, S.; Antony, J.; Ehrlich, S.; Krieg, H. A consistent and accurate ab initio parameterization of density functional dispersion correction (DFT-D) for the 94 elements H-Pu. *J. Chem. Phys.* **2010**, *132*, No. 154104.
(39) Grimme, S.; Ehrlich, S.; Goerigk, L. Effect of the damping function in dispersion corrected density functional theory. *J. Comput. Chem.* **2011**, *32*, 1456−1465.
(40) Frisch, M. J.; Trucks, G. W.; Schlegel, H. B.; Scuseria, G. E.; Robb, M. A.; Cheeseman, J. R.; Scalmani, G.; Barone, V.; Petersson, G. A.; Nakatsuji, H.; Li, X.; Caricato, M.; Marenich, A.; Bloino, J.; Janesko, B. G.; Gomperts, R.; Mennucci, B.; Hratchian, H. P.; Ortiz, J. V.; Izmaylov, A. F.; Sonnenberg, J. L.; Williams-Young, D.; Ding, F.; Lipparini, F.; Egidi, F.; Goings, J.; Peng, B.; Petrone, A.; Henderson, T.; Ranasinghe, D.; Zakrzewski, V. G.; Gao, J.; Rega, N.; Zheng, G.; Liang, W.; Hada, M.; Ehara, M.; Toyota, K.; Fukuda, R.; Hasegawa, J.; Ishida, M.; Nakajima, T.; Honda, Y.; Kitao, O.; Nakai, H.; Vreven, T.; Throssell, K.; Montgomery, J. A., Jr.; Peralta, J. E.; Ogliaro, F.; Bearpark, M.; Heyd, J. J.; Brothers, E.; Kudin, K. N.; Staroverov, V. N.; Keith, T.; Kobayashi, R.; Normand, J.; Raghavachari, K.; Rendell, A.; Burant, J. C.; Iyengar, S. S.; Tomasi, J.; Cossi, M.; Millam, J. M.; Klene, M.; Adamo, C.; Cammi, R.; Ochterski, J. W.; Martin, R. L.; Morokuma, K.; Farkas, O.; Foresman, J. B.; Fox, D. J. *Gaussian 16*, revision B.01; Gaussian, Inc.: Wallingford, CT, 2009.
(41) Hutter, J.; Alavi, A.; Deutsch, T.; Bernasconi, M.; Goedecker, S.; Marx, D.; Tucker-man, M.; Parrinello, M. *CPMD*, version 3.9.1; IBM Research Division, IBM Corp and Max Planck Institute Stuttgart, 2004.
(42) Troullier, N.; Martins, J. L. Efficient Pseudopotentials for Plane-Wave Calculations. *Phys. Rev. B* **1991**, *43*, No. 1993.

DOI: 10.1021/acsomega.8b01615
ACS Omega 2018, 3, 10589−10600